Water Science & Technology

IWA PUBLISHING

Water Science & Technology Vol 84 No 5, 1280 doi: 10.2166/wst.2021.301

Zinc and cadmium adsorption from wastewater using hydroxyapatite synthesized from flue gas desulfurization waste

Sıla Kızıltas Demir and Nurcan Tugrul*

Department of Chemical Engineering, Faculty of Chemical and Metallurgical Engineering, Yildiz Technical University, Davutpasa Campus, Davutpasa Street No. 127, Esenler, 34220 Istanbul, Turkey
*Corresponding author. E-mail: ntugrul@yildiz.edu.tr; ntugrul@hotmail.com

ABSTRACT

The purpose of this work is to produce an alternative cost-effective adsorbent to remove zinc and cadmium from wastewater using hydroxyapatite (HAP) synthesized with hydrothermal method from FGD (Flue gas desulfurization) waste generated by two different coal power plants. The effects of FGD type (Cayırhan and Orhaneli) and molar ratio ($H_3PO_4/CaSO_4$) (0.6–4.79) on HAP synthesis were investigated. Afterwards, effects of the adsorbent dose (1–2 g/L), heavy metal concentration (30, 40, 50 mg/L) and contact time (1, 2, 3, 4 h) on zinc and cadmium adsorption yield from synthetic wastewater using produced HAP were examined. FGD waste and synthesized FGD-HAP were characterized by X-Ray Diffraction (XRD), Fourier Transformed Infrared Spectroscopy (FT-IR), Scanning Electron Microscope (SEM) and Brunauer-Emmett-Teller (BET) instruments. The zinc and cadmium concentration was studied by Inductively coupled plasma atomic emission spectroscopy (ICP-AES). Maximum zinc adsorption capacity of the Cayırhan FGD-HAP was 49.97 and 49.99 mg/L, Orhaneli FGD-HAP was 49.96 and 49.99 mg/L, for 1 g/L and 2 g/L adsorbent dose, respectively, for 50 mg/L heavy metal concentration and 4 h contact time. Maximum cadmium adsorption capacity of the Cayırhan FGD-HAP was 39.98 and 39.99 mg/L, Orhaneli FGD-HAP was 40 and 39.99 mg/L, for 1 g/L and 2 g/L adsorbent dose, respectively, for 40 mg/L heavy metal concentration and 4 h contact time. Adsorption yields were calculated between 98.53% and 100%. The adsorption data were well explained by a second-order kinetic model, and the Freundlich isotherm model fits the equilibrium data. The adsorption results demonstrated that FGD's waste is an effective source to synthesize HAP, which is used as an adsorbent for zinc and cadmium removal from wastewater due to high adsorption capacity.

Key words: adsorption, cadmium, flue gas desulfurization, hydroxyapatite, waste, zinc

HIGHLIGHTS

- An alternative FGD-HAP adsorbent was produced to remove Zn and Cd from wastewater.
- FGD waste generated by coal power plants was used for FGD-HAP synthesis.
- The heterogeneous and porous nature confirms that FGD-HAP is a successful adsorbent.
- The maximum removal efficiency of the FGD-HAPs was calculated between 98.53% and 100%.
- FGD waste pollution was eliminated and FGD waste was changed into valuable product.

GRAPHICAL ABSTRACT

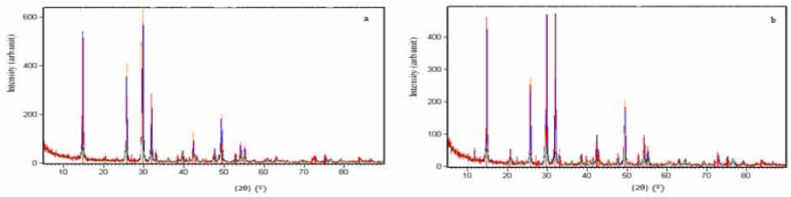

Fig. 1 XRD pattern of FGD waste of coal power plant a) Cayırhan b) Orhaneli

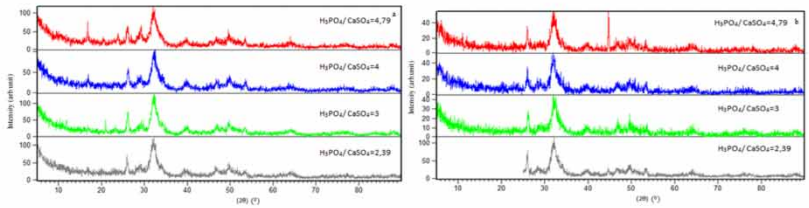

Fig. 2 XRD pattern of FGD-HAP synthesized in different mole ratios from coal power plant a) Cayırhan b) Orhaneli

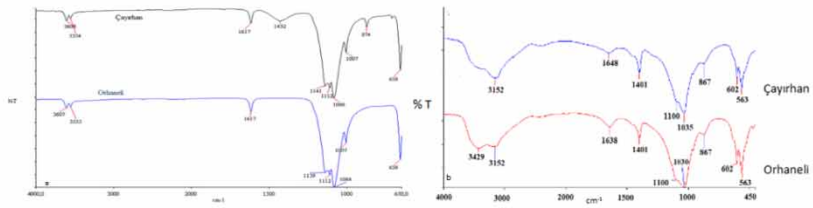

Fig. 3 FT-IR spectrum of a) FGD wastes b) synthesized FGD-HAP

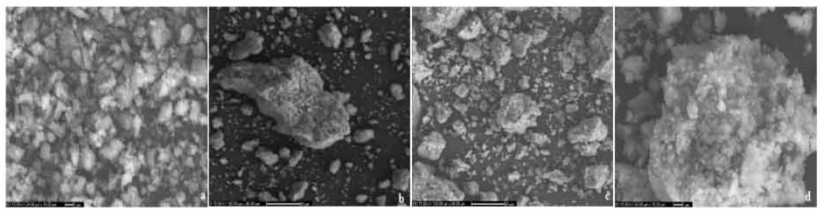

Fig. 4 SEM images of synthesized FGD-HAP a) Cayırhan 1000×magnification b) Cayırhan 5000×magnification c) Orhaneli 1000×magnification d) Orhaneli 5000×magnification

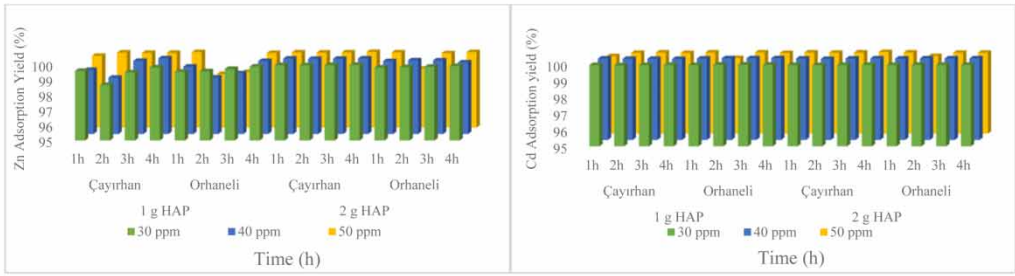

Fig. 5 a) Zn b) Cd adsorption yield of FGD-HAP

INTRODUCTION

Heavy metals such as cadmium, cobalt, zinc, lead, copper, chromium, iron, mercury and arsenic can cause serious health problems and damage the environment, when their concentrations pass the permissible limits (Naushad *et al.* 2015; Jamshaid *et al.* 2017; Saleh *et al.* 2019; Hasanpour & Hatami 2020; Palash *et al.* 2020). With rapid development of industrialization, increasing levels of heavy metals such as zinc and cadmium are discharged to the environment constituting significant danger to the living (Liu *et al.* 2018). Zinc ions are discharged from the fabric, wood, metal coating, mining, ceramic, battery production, drug, sun blocks and deodorant industries and cadmium ions are discharged by the metallurgy, machinery, mining and electroplating industries to wastewater (Ngabura *et al.* 2018; Vardhan *et al.* 2019; Kumar & Pakshirajan 2021). Respiratory, renal, skeletal and cardiovascular system damage and lung, kidney, prostate and stomach cancers appear in children, because of the cadmium toxicity. Zinc is necessary for physiological and metabolic activities of many organisms, but high amounts of zinc can be toxic to them (Kinuthia *et al.* 2020; Palash *et al.* 2020). The US EPA's regulatory cadmium limit is 0.005 mg/L and zinc limit is 5 mg/L in drinking water. The World Health Organization recommended safe limit for cadmium is 0.003 mg/L and for zinc is 3 mg/L in wastewater (Javed & Usmani 2013; Ngabura *et al.* 2018; W.H.O. 2018; Kinuthia *et al.* 2020). Consequently, these heavy metals must be removed from wastewater to preserve human health and the environment. A large number of chemical or physical technologies have been employed, like coagulation, ion exchange, osmosis, photocatalysis, phytoremediation, membrane separation, reverse osmosis, electro floatation, adsorption etc., for waste water remediation (Ihsanullah *et al.* 2015; Jamshaid *et al.* 2017; Sharma & Naushad 2020). Adsorption has been acknowledged as the most economical removal method of zinc and cadmium from wastewater in literature (Yan *et al.* 2014; Chen *et al.* 2020). Hydroxyapatite (HAP) and its composites are utilized as a significant adsorbent for adsorption of many pollutants, like heavy metals, from wastewater (Pai *et al.* 2020). HAP, $Ca_{10}(PO_4)_6(OH)_2$, is one of the most biocompatible inorganic materials used in the human body, and it has shown good binding capacity with metallic ions from wastewater (Ibrahim *et al.* 2020; Jiang *et al.* 2020). HAP can be synthesized using chemical precursors like calcium and phosphorus, using various techniques including, dry, wet and high-temperature methods. Scientists tried to evolve cost-effective calcium sources, instead of using expensive reagents, in order to reduce HAP costs (Liu *et al.* 2018; Mohd Pu'ad *et al.* 2020). Flue gas desulfurization (FGD) gypsum is an industrial by-product produced during the FGD process in coal-fired power plants. Its major composition is $CaSO_4.2H_2O$, so it is an ideal calcium source. A significant amount of FGD waste is discharged directly, which occupies an extensive quantity of land resources and causes high levels of environmental pollution. Therefore, finding a suitable process to change waste FGD to valuable products can be an economical solution to this problem. The precipitation and adsorption yield of FGD waste is high, and it could be used for environmental purposes. Nowadays, phosphate has been used for adsorption and immobilization of heavy metal from water and soil as a cost-effective and environmentally friendly technology. The FGD-HAP exhibited a high efficiency in the removal of aqueous heavy metals. Yan *et al.* (2014) studied Pb^{+2} and Cd^{+2} removal from wastewater using HAP synthesized from FGD waste, and Liu *et al.* (2018) used FGD-HAP to immobilize Pb^{+2} and Cu^{+2} in aqueous solution and soil (Yan *et al.* 2014, 2020; Liu *et al.* 2018; Koralegedara *et al.* 2019; Li *et al.* 2019).

In this study, FGD waste fabricated from two different coal power plants was converted to HAP by hydrothermal method. The aim of this study is to use synthesized FGD-HAP as an alternative low-cost adsorbent to remove zinc and cadmium from wastewater. FGD-HAP synthesis conditions (waste type and $H_3PO_4/CaSO_4$ molar ratio) were determined and the effects of experimental conditions (adsorbent dose, zinc and cadmium concentration, and contact time) on the adsorption performance were examined. FGD waste and synthesized FGD-HAP were characterized by X-Ray Diffraction (XRD), Fourier Transformed Infrared Spectroscopy (FT-IR), Scanning Electron Microscope (SEM) and Brunauer-Emmett-Teller (BET) instruments. The zinc and cadmium concentration was measured by Inductively coupled plasma atomic emission spectroscopy (ICP-AES). Adsorption yields were calculated between 98.53% and 100%. The adsorption data were well explained by a second-order kinetic model and the Freundlich isotherm model fits the equilibrium data. The adsorption results demonstrated that FGD waste is an effective source to synthesize HAP, which is used as an adsorbent for zinc and cadmium removal from wastewater due to high adsorption capacity. The major distinction of this study from previous studies is the use of FGD-HAP synthesized using FGD waste generated by two different coal power plants as an alternative cost-effective adsorbent to remove zinc and cadmium from wastewater, also contributing to environmental preservation and the economy. FGD waste pollution can be eliminated and FGD waste can be changed into valuable product.

MATERIALS AND METHODS

FGD waste used in this study was supplied from Orhaneli (Bursa) and Cayırhan (Ankara) coal-fired power plants in Turkey. The chemical reagents, phosphoric acid (85%) and ammonia solution (25%), used for HAP synthesis, and $Zn(NO_3)_2.6H_2O$ (98%) and $Cd(NO_3)_2.4H_2O$ (99%), used for synthetic wastewater preparation, were purchased from Merck (Darmstadt, Germany).

FDG-HAP Synthesis

FGD waste obtained from two different coal power plants was washed with distilled water and dried at 105 °C for 24 h. Dried FGD waste was crushed in a grinder into fine powder to provide uniformity. FGD-HAP synthesis from FGD wastes was carried out based on Equations (1) and (2). To determine the effect of mole ratio on synthesis yield, determined amounts of waste raw material were mixed in 50 mL of distilled water at 500 rpm for 30 minutes at room temperature. The necessary amount of phosphoric acid was added ($H_3PO_4/CaSO_4$ mole ratio: 0.6, 0.8, 1, 1.2, 2.39, 3, 4, 4.79) and by adding sufficient amount of ammonia solution, the pH of the reaction was made equal to 11. To determine the effect of the pure water amount, preliminary experiments were made with 25, 50 and 100 mL pure water.

$$5\ CaSO_4\ 2H_2O + 3\ H_3PO_4 \rightarrow Ca_5(PO_4)_3 + 5\ H_2SO_4 + 9\ H_2O \quad (1)$$

$$10\ NH_4OH + 5\ H_2SO_4 \rightarrow 5\ (NH_4)_2SO_4 + 10\ H_2O \quad (2)$$

After determining the optimum mole ratio, experiments were performed at various temperatures (20 °C, 30 °C and 40 °C) to identify the temperature effect on the FDG-HAP synthesis. The appropriate time for complete reaction was decided by repeating the experiment at various time intervals (1, 2 and 4 h). The produced FDG-HAP was filtered and was dried at 80 °C for 12 h. The dried product was milled and the product powder was stored in low-density polyethylene bags at room temperature (Mousa & Hanna 2013; Yan *et al.* 2014; Koralegedara *et al.* 2019).

FGD waste and FGD-HAP characterization

The crystalline phases of the FGD waste and synthesized FGD-HAP were analyzed by PANalytical Xpert Pro XRD (PANalytical B.V., Almelo, The Netherlands) at 45 kV and 40 mA, using X-rays produced with Cu-Kα tube. The FT-IR spectra was investigated using a PerkinElmer Spectrum One FT-IR spectrometer (Waltham, MA, USA), equipped with a universal attenuation total reflectance sampling accessory, having spectral range between 4,000 and 650 cm^{-1}. The surface properties and morphology of the synthesized FGD-HAP were examined with an Apollo 300 field-emission SEM (CamScan, Oxford, UK) equipped with a back-scattering electron detector at 15 kV, and 1000× and 5000× magnification was set. The BET surface areas of FGD-HAP adsorbents were measured on a Micromeritics ASAP 2020 instrument using N_2 adsorption after degassing the adsorbent at 300 °C for 3 h. The concentration of zinc and cadmium ions in synthetic wastewater was measured by PerkinElmer Optima 2100 DV ICP-OES equipped with an AS-93 autosampler (PerkinElmer, CT, USA).

Adsorption experiments

Zinc and cadmium adsorption from wastewater was carried out using the synthesized FGD-HAP adsorbent. The stock solutions were prepared by dissolving 30, 40 and 50 mg/L zinc and cadmium solutions (50 mL). Then, 1 or 2 g/L of synthesized FGD-HAP adsorbent was mixed with the stock solution, at initial pH value 5.6 ± 0.1, 500 rpm stirring speed, at room temperature (22 ± 0.5 °C), for 1, 2, 3 or 4 h. The solution was separated from the adsorbent using filter paper at the end of the adsorption experiments. Three replicates were used for the analysis. The concentration of zinc and cadmium ions in synthetic wastewater was measured by ICP-OES. The amount of zinc and cadmium adsorbed and the removal percentage of zinc and cadmium were calculated by applying Equations (3) and (4), respectively.

$$q_e = (C_o - C_e) \times V/M \quad (3)$$

$$\%Removal = (C_o - C_e)/C_o.100 \quad (4)$$

Here, q_e is the amount of zinc and cadmium adsorbed per gram of adsorbent (mg g^{-1}), C_o is the initial zinc and cadmium concentration (mg/L), C_e is the concentration of zinc and cadmium that remained unadsorbed in the solution (mg/L), V is the volume of zinc and cadmium solution (L), and M is the amount of adsorbent (g).

Adsorption studies

Hydroxyapatite (HA) is a perfect sorbent for removal of heavy metals such as Cr, Pb, Cd, Ni, Zn, Al, Cu, Fe, Co, Mn, and Fe, having excellent properties like: non-toxic, inexpensive and readily available, high adsorption capacity, low water solubility, and high stability under reducing and oxidizing conditions. The overall removal of Zn and Cd by HA appears to be due to a two-step mechanism. The first step involves the rapid surface complexation of Zn and Cd ions on the surface of HA particles. In the second step the diffusion of metal ions within the HA particles through the ion exchange with Ca occurs, leading to the formation of a Zn and Cd-containing HA. The complexation of Zn and Cd on the HA surface partially removed the H^+ ions, explaining pH decrease and calcium release. This mechanism can be expressed by the following general reaction (Corami *et al.* 2007, 2008; Ibrahim *et al.* 2020):

$$HA{-}OH + Cd^{2+} = HA{-}O{-}Cd^{+} + H^{+} \quad (5)$$

$$HA{-}OH + Zn^{2+} = HA{-}O{-}Zn^{+} + H^{+} \quad (6)$$

RESULTS AND DISCUSSION

Characterization of the FGD waste and synthesized FGD-HAP

XRD patterns of Cayırhan and Orhaneli FGD wastes are shown in Figure 1. According to the XRD results, Cayırhan FGD waste was identified as a mixture of bassanite (pdf. no: 00-033-0310; $CaSO_4.1/2H_2O$) and calcite (pdf. no: 00-001-0837; $CaCO_3$), and Orhaneli FGD waste was identified as a mixture of bassanite (pdf. no: 00-033-0310; $CaSO_4.1/2H_2O$) and gypsum (pdf. no: 01-074-1433; $CaSO_4.2H_2O$). The high ratio of calcium in both compounds found in the structure indicates that they can be used in the synthesis of HAP. The peaks observed in the XRD pattern at 15°, 30°, 40° and 50° are characteristic peaks of HAP (Hokkanen *et al.* 2018).

XRD patterns of synthesized FGD-HAP were measured at different H_3PO_4/FGD mole ratios, reaction temperatures and reaction times. The XRD score of a compound can be defined by the similarity of the peak intensities (%) and locations of the phase to the pdf card pattern of the reference mineral. A continuous increase was observed until the mole ratio was equal to 4; when the mole ratio was equal to 4.79 the XRD scores decreased. This situation indicated that increasing H_3PO_4/FGD mole ratio in reaction medium contributed to the FGD-HAP formation until the mole ratio was equal to 4, and with the decreasing H_3PO_4/FGD mole ratio, XRD scores of samples were increased dramatically. Due to the highest XRD scores for both wastes, the H_3PO_4/FGD mole ratio of 4:1 was selected as optimum (Figure 2). Table 1 shows XRD scores of synthesized FGD-HAP, where only pure HAP was observed. This confirms that pure HAP was synthesized successfully. As a result of the preliminary experiments, it has been observed that temperature and time did not affect the FDG-HAP synthesis efficiency (Mousa & Hanna 2013; Zhang *et al.* 2016; Sari *et al.* 2017).

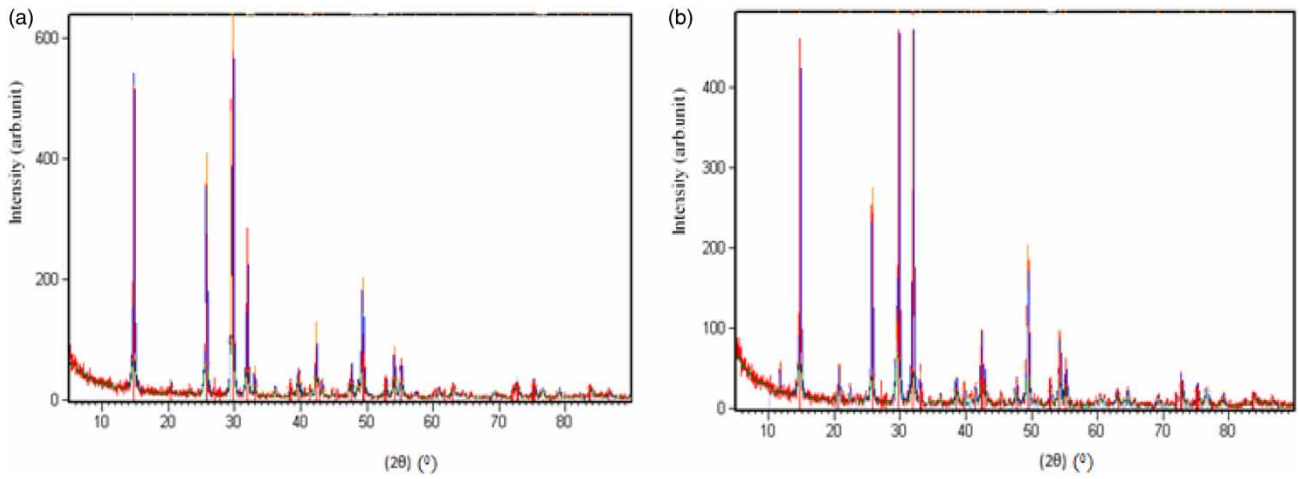

Figure 1 | XRD pattern of FGD waste of coal power plant (a) Cayırhan (b) Orhaneli.

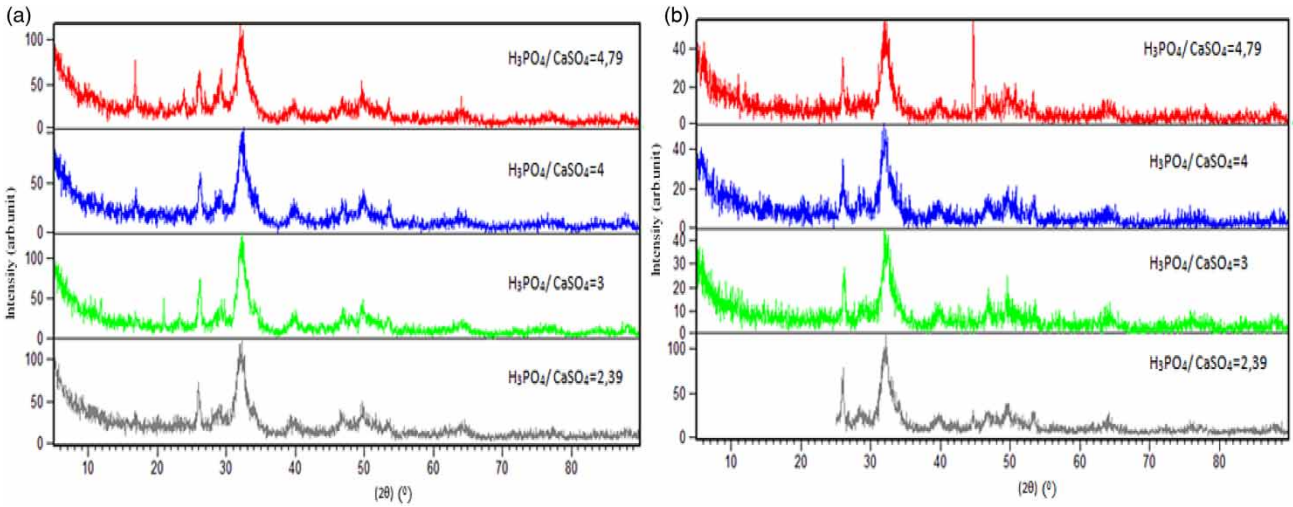

Figure 2 | XRD pattern of FGD-HAP synthesized in different mole ratios from coal power plant (a) Cayırhan (b) Orhaneli.

Table 1 | XRD scores of the FGD-HAP synthesized with different H_3PO_4/FGD mole ratios

H_3PO_4/FGD mole ratios	Pdf no.	Mineral name	Chemical formula	Cayırhan score	Orhaneli score
2.39	00-001-1008	Hydroxyapatite	$Ca_{10}(PO_4)_6(OH)_2$	41	34
3	00-001-1008	Hydroxyapatite	$Ca_{10}(PO_4)_6(OH)_2$	45	40
4	00-001-1008	Hydroxyapatite	$Ca_{10}(PO_4)_6(OH)_2$	50	47
4.79	00-001-1008	Hydroxyapatite	$Ca_{10}(PO_4)_6(OH)_2$	27	25

The FT-IR spectra of Cayırhan and Orhaneli FGD wastes are shown in Figure 3(a). The peaks seen at 3,608–3,554 cm^{-1} (Cayırhan) and 3,607–3,553 cm^{-1} (Orhaneli) were related to the O-H stretching and H_2O bending vibration of basanite. The band at 1,617 cm^{-1} could be ascribed to the H-OH bonding in water. The peaks observed between 1,007 and 1,141 cm^{-1} belong to SO_4^{2-} vibration bands. The band observed at 874 cm^{-1} was assigned to the CO_3 group. The peak seen at 658 cm^{-1} is the characteristic peak of $CaSO_4$ (Kang *et al.* 2019). Figure 3(b) represented the FT-IR spectrum of synthesized FGD-HAP. The peak at 3,429 cm^{-1} (Orhaneli FGD-HAP) was assigned to hydroxyl groups. The peaks at 3,152, 1,648 (Cayırhan FGD-HAP) and 1,638 cm^{-1} (Orhaneli FGD-HAP) can be attributed to the adsorbed water. The peaks at 563, 602, 1,035 (Cayırhan FGD-HAP), 1,030 (Orhaneli FGD-HAP) and 1,100 cm^{-1} corresponded to the stretching vibration of the phosphate groups. The peaks observed at 1,401 and 867 cm^{-1} correspond to the carbonate groups, demonstrating carbonate partially substituted for the phosphate while FGD-HAP is subjected to atmosphere. The 1,401 cm^{-1} peak may also be due to atmospheric carbon dioxide from the air environment in the preparation phase. The signals of synthesized FGD-HAP coincided to a great extent with the major absorbance signals of HAP (El Asri *et al.* 2010; Salah *et al.* 2014; Yan *et al.* 2014; El-Zahhar & Awwad 2016; Zou *et al.* 2019; Jiang *et al.* 2020).

The surface morphology of FGD-HAP particles synthesized from Cayırhan and Orhaneli FGD wastes was examined by SEM at 1000× and 5000× magnification. The SEM images obtained are given in Figure 4. The synthesized FGD-HAP surface, has a medium grain size porous surface structure which provides a suitable area for zinc and cadmium adsorption from wastewater. The reason for this morphology is the presence of the CO_3 group and the high calcium content, which limit the growth of FGD-HAP crystals. The small particle size increases the specific surface area and the porous structure allows adsorption not only on the surface but also between the pores. As a result, synthesized FGD-HAP has high adsorption properties (El-Zahhar & Awwad 2016; Deb *et al.* 2019; Liu *et al.* 2021). The BET surface area of Cayırhan FGD-HAP was 85.224 m^2/g and Orhaneli FGD-HAP was 82.652 m^2/g. The high surface area of FGD-HAP has proved that it can be used in zinc and cadmium adsorption process.

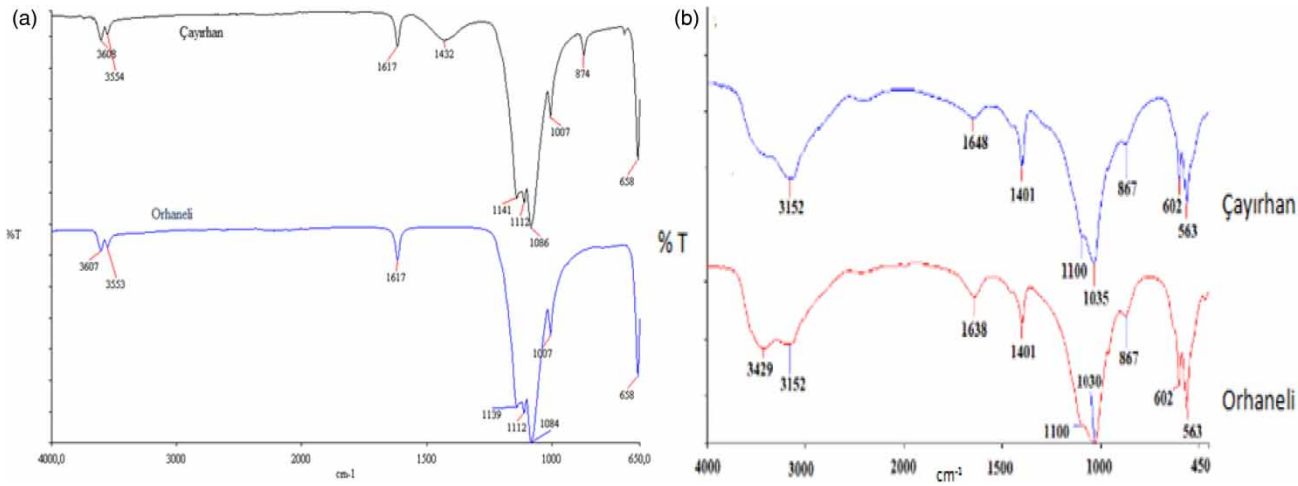

Figure 3 | FT-IR spectrum of (a) FGD wastes, (b) synthesized FGD-HAP.

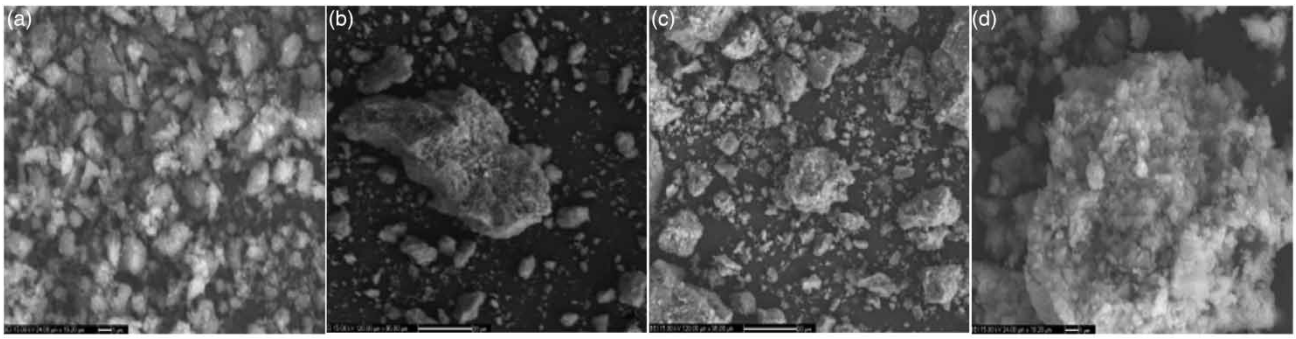

Figure 4 | SEM images of synthesized FGD-HAP: (a) Cayırhan 1000 × magnification, (b) Cayırhan 5000 × magnification, (c) Orhaneli 1000 × magnification, (d) Orhaneli 5000 × magnification.

Adsorption analysis results

Heavy metals like cadmium, zinc, lead, nickel, copper, mercury and chromium are primary pollutants in industrial wastewaters, causing a serious risk to public health and the environment when they exceed the permissible limits (Saleh *et al.* 2019; Turkmen Koc *et al.* 2020). The use of FGD-HAP as an adsorbent for zinc and cadmium was realized by conversion of waste FGD to HAP with hydrothermal method. Then, 1 or 2 g/L of synthesized FGD-HAP adsorbent was mixed with a stock solution. The stock solutions were prepared from standard zinc and cadmium solutions with concentrations of 30, 40 and 50 mg/L. For the adsorption experiments, 50 mL of treatment solution was used with 500 rpm stirring speed, at room temperature (22 $\pm$ 0.5 °C), for 1, 2, 3 or 4 h. The solution was separated from the adsorbent using filter paper at the end of the adsorption experiments. Experiments were repeated three times. The concentration of zinc and cadmium was measured by ICP-OES. The results of analyses are given in Figure 5. The maximum zinc and cadmium removal efficiency of the FGD-HAPs was calculated between 98.53% and 100%. The zinc adsorption capacity of Cayırhan FGD-HAP was higher than Orhaneli FGD-HAP, but on the contrary, the cadmium adsorption capacity of Cayırhan FGD-HAP was lower than Orhaneli FGD-HAP. The adsorption efficiency increases when the amount of adsorbent increases. This increase could be explained by an increased number of active sites for zinc and cadmium adsorption on the HAP surface (Ivanets *et al.* 2019; Long *et al.* 2019; Jiang *et al.* 2020).

A comparison of maximum monolayer adsorption capacity of zinc and cadmium of various adsorbents is shown in Table 2. The maximum monolayer adsorption capacity of FGD-HAP is higher than the other adsorbents shown in Table 2.

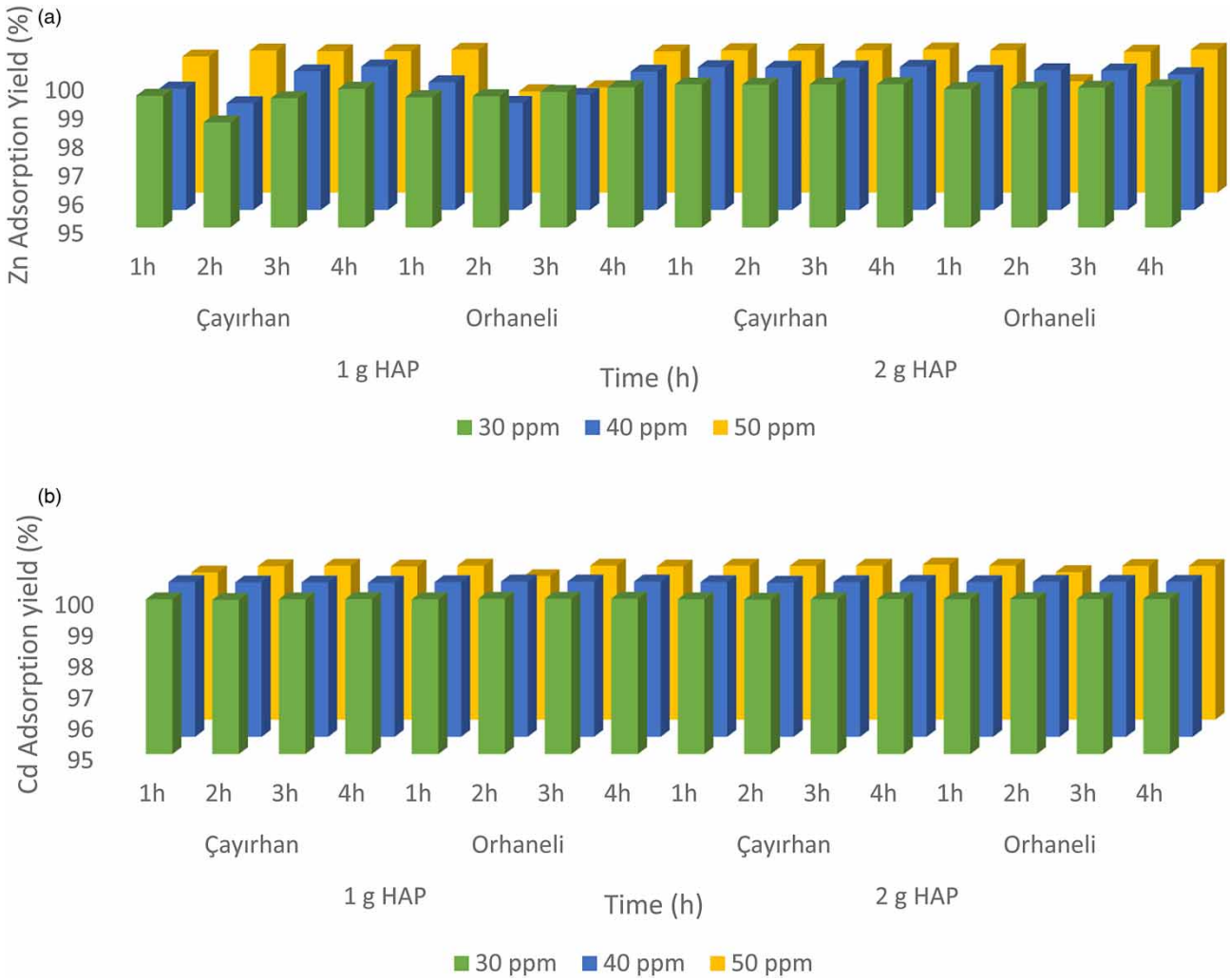

Figure 5 | (a) Zn^{+2} (b) Cd^{+2} adsorption yield of FGD-HAP.

Table 2 | Comparison of maximum adsorption capacity of Zn^{+2} and Cd^{+2} on various adsorbents

	Maximum adsorption capacity (mg g^{-1})		
Adsorbents	**Zn^{+2}**	**Cd^{+2}**	**References**
HAP	1.17		Corami *et al.* (2007)
HAP	–	2.58	Corami *et al.* (2008)
FGD-HAP	–	43.10	Yan *et al.* (2014)
Carbon nanotubes	–	2.02	Ihsanullah *et al.* (2015)
HCl modified durian peels	36.73	–	Ngabura *et al.* (2018)
Corn stalk (CB)	–	40	Chen *et al.* (2020)
FGD-HAP	49.99		Present study
FGD-HAP		39.99	Present study

Sorption kinetics

Pseudo-first-order and pseudo-second-order kinetic models were applied to define the kinetic order of the zinc and cadmium adsorption by FGD-HAP. These are given in the following (Zhang *et al.* 2016; Ivanets *et al.* 2019; Long *et al.* 2019).

Pseudo-first-order equation: $$q_t = q_e(1 - e^{-k_1 t}) \tag{7}$$

Pseudo-second-order equation: $$q_t = \frac{k_2 q_e^2 t}{1 + k_2 q_e t} \tag{8}$$

where q_t and q_e are the amounts of zinc and cadmium adsorbed at time t and at equilibrium (mg g^{-1}), respectively, k_1 is the rate constant of pseudo-first-order adsorption process (g mg^{-1} min^{-1}), and k_2 is the equilibrium rate constant of pseudo-second-order adsorption (g mg^{-1} min^{-1}) (Mohammadi *et al.* 2020; Afshin *et al.* 2021). The pseudo-second-order kinetic parameters, which are a better fit with the adsorption of zinc and cadmium on the FGD-HAP, are given in Figure 6.

Sorption isotherms

Langmuir and Freundlich adsorption isotherms, the most frequently used models to demonstrate liquid phase adsorption equilibrium data, were employed to examine the adsorption behaviors of FGD-HAP. The Langmuir equation is expressed as follows (Dehghan *et al.* 2019; Yousefi *et al.* 2021):

$$\frac{C_e}{q_e} = \frac{1}{Q_{max} K} + \frac{C_e}{Q_{max}} \tag{9}$$

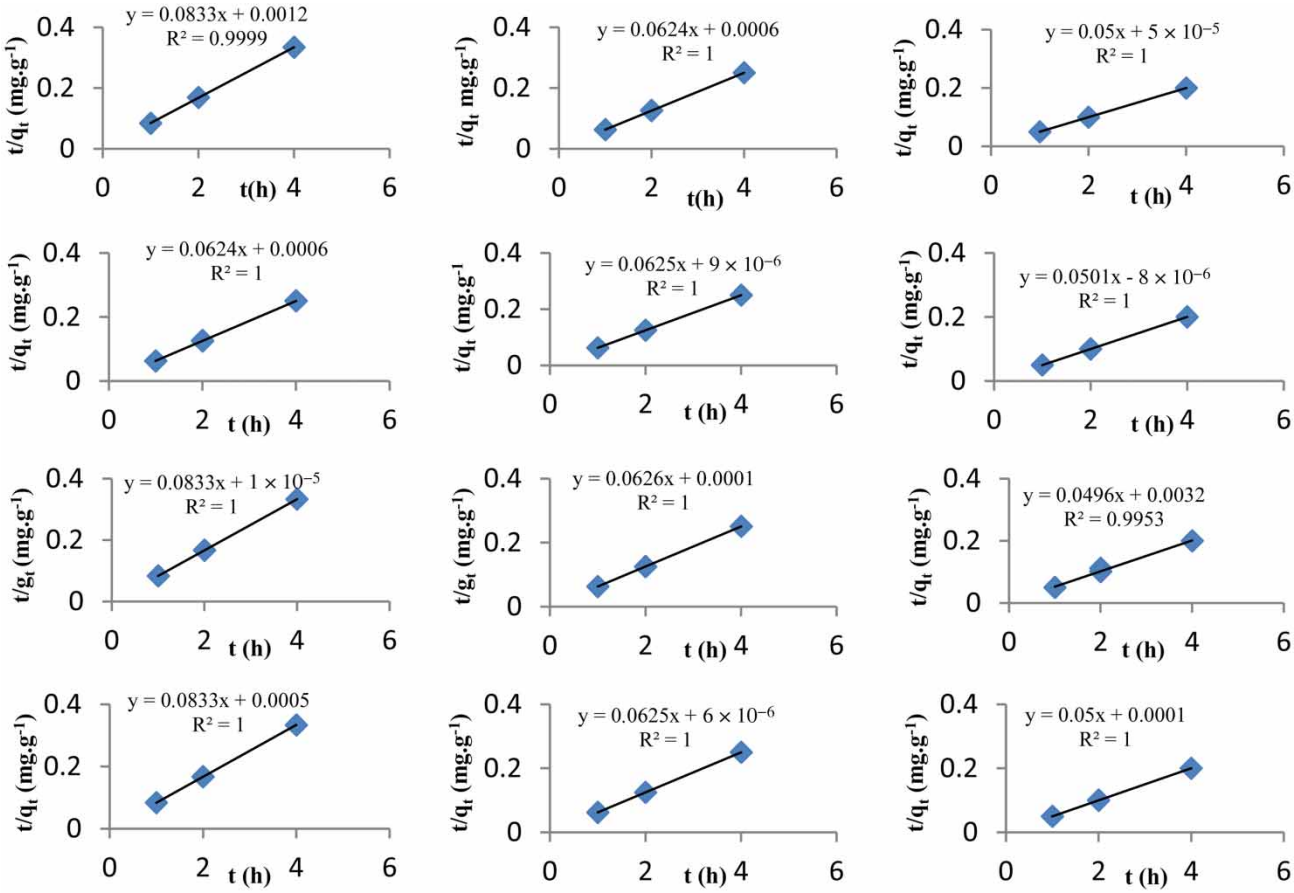

Figure 6 | The pseudo-second-order kinetic model for the Zn^{+2} and Cd^{+2} adsorption on the FGD-HAP.

q_e is the adsorption quantity per unit mass of adsorbent in equilibrium (mg. g^{-1}) and Q_{max} (mg. g^{-1}) is the maximum adsorption capacity, K (L.mg^{-1}) is the Langmuir constant, and C_e is the equilibrium concentration. A linear plot can be obtained when C_e/q_e is plotted against C_e over the concentration range of zinc and cadmium.

The Freundlich equation is expressed as follows:

$$\ln q_e = \ln K_F + \frac{1}{n} \ln C_e \tag{10}$$

where K_F is the adsorption capacity (mg. g^{-1}) and n is the adsorption intensity. The Freundlich parameters K_F and n are determined by plotting the relationship between ln q_e and ln C_e. The Langmuir isotherm defines the monolayer formation during adsorption of an adsorbate on a homogeneous surface, while the Freundlich isotherm indicates the adsorption mechanism on a heterogeneous surface (Yan *et al.* 2014; Hokkanen *et al.* 2018; Jing *et al.* 2018; Liu *et al.* 2018; Ain *et al.* 2020).

The results in Table 3 indicate that the Freundlich isotherms fits better with the experimental data than Langmuir, proposing a better R^2 value. This result proves the heterogeneous and porous nature of the FGD-HAP adsorbents. The adsorption in this study is a series process of multilayer adsorption. The value of n greater than 1 ($n > 1$) in the Freundlich model indicates that the conditions were favorable and the FGD-HAP is an encouraging adsorbent to remove zinc and cadmium from wastewater. These results confirmed that Cayırhan FGD-HAP is more effective for zinc and cadmium adsorption.

CONCLUSIONS

In this study, low-cost adsorbent synthesized using FGD waste generated by Cayırhan and Orhaneli coal power plants was used for zinc and cadmium adsorption from wastewater, FGD waste pollution was eliminated and FGD waste was changed into valuable product. FGD waste and synthesized FGD-HAP were characterized by XRD, FT-IR, SEM and BET devices. The results are summarized as follows:

Table 3 | The results of Langmuir and Freundlich adsorption model analysis

FGD type	Metal type	Adsorbent amount (g)	Wastewater concentration (mg/L)	Langmuir	Freundlich		
				R^2	K_f	n	R^2
Cayırhan	Zn^{+2}	1	30	0.7426	0.9940	2.467	0.9337
			40	0.8423	0.9980	2.760	0.8922
			50	0.8846	0.9980	2.990	0.9805
		2	30	0.9994	0.9970	2.475	0.9999
			40	0.9931	0.9980	2.766	0.9983
			50	0.9774	0.9990	2.992	0.9951
	Cd^{+2}	1	30	0.9999	0.0001	2.484	0.9999
			40	0.9031	0.9986	2.990	0.9999
			50	0.6868	0.0001	2.484	0.9999
		2	30	0.9999	0.0001	2.484	0.9999
			40	0.6925	0.0002	2.772	0.8449
			50	0.3989	0.9999	2.994	0.5741
Orhaneli	Zn^{+2}	1	30	0.9958	0.9975	2.4755	0.9984
			40	0.9951	0.9967	2.7622	0.9983
			50	0.4964	0.9974	2.9834	0.9449
		2	30	0.8185	0.9977	2.476	0.9609
			40	0.9556	0.9981	2.7658	0.9885
			50	0.5484	0.9809	2.9200	0.9593
	Cd^{+2}	1	30	0.9999	0.9977	2.4843	0.9999
			40	0.9999	0.9970	2.7722	0.9999
			50	0.7889	0.9985	2.9895	0.9659
		2	30	0.9999	0.9977	2.4843	0.9999
			40	0.8409	0.9970	2.7722	0.9612
			50	0.6351	0.9991	2.9916	0.9135

1. Optimum H_3PO_4/FGD mole ratio was selected 4:1 because of the high XRD scores.
2. It was seen from FT-IR spectra of FGD-HAP that HAP was synthesized succesfully from FGD waste.
3. It was seen from SEM images of the synthesized FGD-HAP that the adsorbent surface has a medium grain size porous surface structure providing a suitable area for zinc and cadmium adsorption from wastewater. The BET analysis results also support this outcome.
4. Either 1 or 2 g/L of synthesized FGD-HAP adsorbent was mixed with a stock solution prepared by dissolving 30, 40 or 50 mg/L zinc or cadmium solutions for 1, 2, 3 or 4 h. The zinc and cadmium concentrations were determined by ICP-AES. The maximum removal efficiency of the FGD-HAPs was calculated between 98.53% and 100%. The zinc adsorption capacity of Cayırhan FGD-HAP was higher than Orhaneli FGD-HAP, but on the contrary, the cadmium adsorption capacity of Cayırhan FGD-HAP was lower than Orhaneli FGD-HAP. The adsorption efficiency increases when the amount of adsorbent increases.
5. Kinetic studies showed that the second-order kinetic model explains the adsorption process with a high correlation coefficient. The Freundlich isotherm model gives the best result to the equilibrium experimental data.

This result proves the heterogeneous and porous nature of the FGD-HAP confirming that FGD-HAP, is a successful adsorbent for removal of zinc and cadmium from wastewater and Cayırhan FGD-HAP is more effective for zinc and cadmium adsorption. Based on the results of the present work, FGDs waste can be used as an effective source to produce FGD-HAP, which is used as an economical adsorbent for the treatment of wastewaters containing zinc and cadmium metal ions because of its excellent adsorption performance. Using the produced adsorbent in industrial wastewater for adsorption of different heavy metals can be recommended for future research. Besides, in this study, the adsorption capacity of FGD-HAP is studied from a single-component solution for zinc and cadmium. FGD-HAP adsorption capacity studies for multi-metal solutions must be done in future studies.

ACKNOWLEDGEMENT

This study was supported by project 2015-07-01-YL04 of Yıldız Technical University Scientific Research Projects Coordinator.

DATA AVAILABILITY STATEMENT

All relevant data are included in the paper or its Supplementary Information.

REFERENCES

Afshin, S., Rashtbari, Y., Vosough, M., Dargahi, A., Fazlzadeh, M., Behzad, A. & Yousefi, M. 2021 Application of Box–Behnken design for optimizing parameters of hexavalent chromium removal from aqueous solutions using Fe_3O_4 loaded on activated carbon prepared from alga: kinetics and equilibrium study. *Journal of Water Process Engineering* **42**, 102113.

Ain, Q. U., Zhang, H., Yaseen, M., Rasheed, U., Liu, K., Subhan, S. & Tong, Z. 2020 Facile fabrication of hydroxyapatite-magnetite-bentonite composite for efficient adsorption of Pb(II), Cd(II), and crystal violet from aqueous solution. *Journal of Cleaner Production* **247**, 119088.

Chen, G., Wang, C., Tian, J., Liu, J., Ma, Q., Liu, B. & Li, X. 2020 Investigation on cadmium ions removal from water by different raw materials-derived biochars. *Journal of Water Process Engineering* **35**, 101223.

Corami, A., Mignardi, S. & Ferrini, V. 2007 Copper and zinc decontamination from single- and binary-metal solutions using hydroxyapatite. *Journal of Hazardous Materials* **146**, 164–170.

Corami, A., Mignardi, S. & Ferrini, V. 2008 Cadmium removal from single- and multi-metal (Cd + Pb + Zn + Cu) solutions by sorption on hydroxyapatite. *Journal of Colloid and Interface Science* **317**, 402–408.

Deb, P., Barua, E., Lala, S. D. & Deoghare, A. B. 2019 Synthesis of hydroxyapatite from *Labeo rohita* fish scale for biomedical application. *Materials Today* **15** (2), 277–283.

Dehghan, A., Mohammadi, A. A., Yousefi, M., Najafpoor, A. A., Shams, M. & Rezania, S. 2019 Enhanced kinetic removal of ciprofloxacin onto metal-organic frameworks by sonication, process optimization and metal leaching study. *Nanomaterials* **9** (10), 1422.

El Asri, S., Laghzizil, A., Coradin, T., Saoiabi, A., Alaoui, A. & M'hamedi, R. 2010 Conversion of natural phosphate rock into mesoporous hydroxyapatite for heavy metals removal from aqueous solution. *Colloids and Surfaces A: Physicochemical and Engineering Aspects* **362** (1–3), 33–38.

El-Zahhar, A. A. & Awwad, N. S. 2016 Removal of malachite Green dye from aqueous solutions using organically modified hydroxyapatite. *Journal of Environmental Chemical Engineering* **4** (1), 633–638.

Hasanpour, M. & Hatami, M. 2020 Application of three dimensional porous aerogels as adsorbent for removal of heavy metal ions from water/wastewater: a review study. *Advances in Colloid and Interface Science* **284**, 102247.

Hokkanen, S., Bhatnagar, A., Srivastava, V., Suorsa, V. & Sillanpää, M. 2018 Removal of Cd^{2+}, Ni^{2+} and PO_4^{3-} from aqueous solution by hydroxyapatite-bentonite clay-nanocellulose composite. *International Journal of Biological Macromolecules* **118**, 903–912.

Ibrahim, M., Labaki, M., Giraudon, J. M. & Lamonier, J. F. 2020 Hydroxyapatite, a multifunctional material for air, water and soil pollution control: a review. *Journal of Hazardous Materials* **383**, 121139.

Ihsanullah, Al-Khaldi, F. A., Abusharkh, B., Khaled, M., Atieh, M. A., Nasser, M. S., laoui, T., Saleh, T. A., Agarwal, S., Tyagi, I. & Gupta, V. K. 2015 Adsorptive removal of cadmium(II) ions from liquid phase using acid modified carbon-based adsorbents. *Journal of Molecular Liquids* **204**, 255–263.

Ivanets, A. I., Kitikova, N. V., Shashkova, I. L., Roshchina, M. Y., Srivastava, V. & Sillanpää, M. 2019 Adsorption performance of hydroxyapatite with different crystalline and porous structure towards metal ions in multicomponent solution. *Journal of Water Process Engineering* **32**, 100963.

Jamshaid, A., Hamid, A., Muhammad, N., Naseer, A., Ghauri, M., Iqbal, J., Rafiq, S. & Shah, N. S. 2017 Cellulose-based materials for the removal of heavy metals from wastewater – an overview. *ChemBioEng Reviews* **4** (4), 1–18.

Javed, M. & Usmani, N. 2013 Assessment of heavy metal (Cu, Ni, Fe, Co, Mn, Cr, Zn) pollution in effluent dominated rivulet water and their effect on glycogen metabolism and histology of *Mastacembelus armatus*. *Springerplus* **2** (390), 1–13.

Jiang, J., Long, Y., Hu, X., Hu, J., Zhu, M. & Zhou, S. 2020 A facile microwave-assisted synthesis of mesoporous hydroxyapatite as an efficient adsorbent for Pb^{2+} adsorption. *Journal of Solid State Chemistry* **289**, 121491.

Jing, N., Zhou, A. N. & Xu, Q. H. 2018 The synthesis of super-small nano hydroxyapatite and its high adsorptions to mixed heavy metallic ions. *Journal of Hazardous Materials* **353**, 89–98.

Kang, J., Gou, X., Hu, Y., Sun, W., Liu, R., Gao, Z. & Guan, Q. 2019 Efficient utilisation of flue gas desulfurization gypsum as a potential material for fluoride removal. *Science of the Total Environment* **649**, 344–352.

Kinuthia, G. K., Ngure, V., Beti, D., Lugalia, R., Wangila, A. & Kamau, L. 2020 Levels of heavy metals in wastewater and soil samples from open drainage channels in Nairobi, Kenya: community health implication. *Scientific Reports* **10**, 8434.

Koralegedara, N. H., Pinto, P. X., Dionysiou, D. D. & Al-Abed, S. R. 2019 Recent advances in flue gas desulfurization gypsum processes and applications – a review. *Journal of Environmental Management* **251**, 109572.

Kumar, M. & Pakshirajan, K. 2021 Continuous removal and recovery of metals from wastewater using inverse fluidized bed sulfidogenic bioreactor. *Journal of Cleaner Production* **284**, 124769.

Li, R., Li, Q., Sun, X., Li, J., Shen, J., Han, W. & Wang, L. 2019 Efficient and rapid removal of EDTA-chelated Pb(II) by the Fe(III)/flue gas desulfurization gypsum (FGDG) system. *Journal of Colloid and Interface Science* **542**, 379–386.

Liu, Y., Yan, Y., Seshadri, B., Qi, F., Xu, Y., Bolan, N., Zheng, F., Sun, X., Han, W. & Wang, L. 2018 Immobilization of lead and copper in aqueous solution and soil using hydroxyapatite derived from flue gas desulphurization gypsum. *Journal of Geochemical Exploration* **184** (B), 239–246.

Liu, Y., Liu, M., Ji, S., Zhang, L., Cao, W., Wang, H. & Wang, S. 2021 Preparation and application of hydroxyapatite extracted from fish scale waste using deep eutectic solvents. *Ceramics International* **47** (7:A), 9366–9372.

Long, Y., Jiang, J., Hu, J., Hu, X., Yang, Q. & Zhou, S. 2019 Removal of Pb(II) from aqueous solution by hydroxyapatite/carbon composite: preparation and adsorption behavior. *Colloids and Surfaces A: Physicochemical and Engineering Aspects* **577**, 471–479.

Mohammadi, A. A., Dehghani, M. H., Mesdaghinia, A., Yaghmaian, K. & Es'haghi, Z. 2020 Adsorptive removal of endocrine disrupting compounds from aqueous solutions using magnetic multi-wall carbon nanotubes modified with chitosan biopolymer based on response surface methodology: functionalization, kinetics, and isotherms studies. *International Journal of Biological Macromolecules* **155**, 1019–1029.

Mohd Pu'ad, N. A. S., Abdul Haq, R. H., Mohd Noh, H., Abdullah, H. Z., Idris, M. I. & Lee, T. C. 2020 Synthesis method of hydroxyapatite: a review. *Materials Today: Proceedings* **29** (1), 233–239.

Mousa, S. & Hanna, A. 2013 Synthesis of nano-crystalline hydroxyapatite and ammonium sulfate from phosphogypsum waste. *Materials Research Bulletin* **48** (2), 823–828.

Naushad, M., Mittal, A., Rathore, M. & Gupta, V. 2015 Ion-exchange kinetic studies for Cd(II), Co(II), Cu(II), and Pb(II) metal ions over a composite cation exchanger. *Desalination and Water Treatment* **54** (10), 2883–2890.

Ngabura, M., Hussain, S. A., Ghani, W. A., Jami, M. S. & Tan, Y. P. 2018 Utilization of renewable durian peels for biosorption of zinc from wastewater. *Journal of Environmental Chemical Engineering* **6** (2), 2528–2539.

Pai, S., Kini, S. M., Selvaraj, R. & Pugazhendhi, A. 2020 A review on the synthesis of hydroxyapatite, its composites and adsorptive removal of pollutants from wastewater. *Journal of Water Process Engineering* **38**, 101574.

Palash Md, A. U., Islam Md, S., Bayero, A. S., Taqui, S. N. & Koki, I. B. 2020 Evaluation of trace metals concentration and human health implication by indigenous edible fish species consumption from Meghna River in Bangladesh. *Environmental Toxicology and Pharmacology* **80**, 103440.

Salah, T. A., Mohammad, A. M., Hassan, M. A. & El-Anadouli, B. E. 2014 Development of nano-hydroxyapatite/chitosan composite for cadmium ions removal in wastewater treatment. *Journal of the Taiwan Institute of Chemical Engineers* **45** (4), 1571–1577.

Saleh, H. N., Panahande, M., Yousefi, M., Asghari, F. B., Conti, G. O., Talaee, E. & Mohammadi, A. A. 2019 Carcinogenic and non-carcinogenic risk assessment of heavy metals in groundwater wells in Neyshabur Plain, Iran. *Biological Trace Element Research* **190**, 251–261.

Sari, S., Senberber, F. T., Yildirim, M., Kipcak, A. S., Aydin, Y. S. & Moroydor, D. E. 2017 Lanthanum borate synthesis via the solid-state method from a La_2O_3 precursor: electrical and optical properties. *Materials Chemistry and Physics* **200**, 196–203.

Sharma, G. & Naushad, M. 2020 Adsorptive removal of noxious cadmium ions from aqueous medium using activated carbon/zirconium oxide composite: isotherm and kinetic modelling. *Journal of Molecular Liquids* **310**, 113025.

Turkmen Koc, S. N., Kipcak, A. S., Derun, E. M. & Tugrul, N. 2020 Removal of zinc from wastewater using orange, pineapple and pomegranate peels. *International Journal of Environmental Science and Technology*. doi.org/10.1007/s13762-020-03025-z.

Vardhan, K. H., Kumar, P. S. & Panda, R. C. 2019 A review on heavy metal pollution, toxicity and remedial measures: current trends and future perspectives. *Journal of Molecular Liquids* **290**, 111197.

World Health Organization (W.H.O.) 2018 *A Global Overview of National Regulations and Standards for Drinking-Water Quality*. World Health Organization, Geneva, pp. 10–76.

Yan, Y., Dong, X., Sun, X., Sun, X., Li, J., Shen, J., Han, W., Liu, X. & Wang, L. 2014 Conversion of waste FGD gypsum into hydroxyapatite for removal of Pb^{2+} and Cd^{2+} from wastewater. *Journal of Colloid and Interface Science* **429**, 68–76.

Yan, Y., Li, Q., Yang, J., Zhou, S., Wang, L. & Boland, N. 2020 Evaluation of hydroxyapatite derived from flue gas desulphurization gypsum on simultaneous immobilization of lead and cadmium in contaminated soil. *Journal of Hazardous Materials* **400**, 123038.

Yousefi, M., Gholami, M., Oskoei, V., Mohammadi, A. A., Baziar, M. & Esrafili, A. 2021 Comparison of LSSVM and RSM in simulating the removal of ciprofloxacin from aqueous solutions using magnetization of functionalized multi-walled carbon nanotubes: process optimization using GA and RSM techniques. *Journal of Environmental Chemical Engineering* **9** (4), 105677.

Zhang, W., Wang, F., Wang, P., Lin, L., Zhao, Y., Zou, P., Zhao, M., Chen, H., Liu, Y. & Zhang, Y. 2016 Facile synthesis of hydroxyapatite/yeast biomass composites and their adsorption behaviors for lead (II). *Journal of Colloid and Interface Science* **477**, 181–190.

Zou, X., Zhao, Y. & Zhang, Z. 2019 Preparation of hydroxyapatite nanostructures with different morphologies and adsorption behavior on seven heavy metals ions. *Journal of Contaminant Hydrology* **226**, 103538.

First received 4 April 2021; accepted in revised form 17 July 2021. Available online 29 July 2021